

UNIVERSITY OF TARTU
Faculty of Science and Technology
Institute of Technology

Avishan Aghayari

Analysis of Clb6 degradation mechanisms

Bachelor's Thesis (12 ECTS)

Curriculum Science and Technology

Supervisor(s):
Assoc. Prof., PhD Ilona Faustova
MSc Artemi Maljavin

Tartu 2022

Analysis of Clb6 degradation mechanisms

Abstract:

Cell cycle is a highly regulated, multi-step process, controlled by cyclin-dependent kinases (Cdk). In yeast, this process is divided into four phases: G1, S, G2, and M. Cdk1 or the master regulator of the cell cycle is responsible for regulating the progression through the different stages of this process. Cyclins bind to Cdk1 and promote its catalytic activity. It has been shown that different cyclins promote phosphorylation of different target substrates. Cyclins are synthesized and degraded in a specific manner to ensure correct progression through the cell cycle. Clb5 and Clb6 are S phase cyclins that regulate DNA replication and other S phase processes. Despite having similarities in their amino acid sequences, they show different expression profiles throughout the cell cycle. Clb5 levels stay stable until mitosis, whereas Clb6 levels drop in the early stages of the S phase. This suggests that Clb6 has a different degradation mechanism compared to Clb5. The goal of this work was to investigate the degradation of Clb6.

Keywords:

cell cycle, cyclin, cyclin-dependent kinase, docking motifs, phospho-degron, phosphorylation, protein degradation,

CERCS: P310 Proteins, Enzymology

Clb6 degradatsiooni mehhanismide analüüs

Lühikokkuvõte:

Rakutsükkel on väga täpselt reguleeritud protsess, mis on pagaripärmis jagatud neljaks faasiks: G1, S, G2 ja M. Seda protsessi reguleerivad tsükliin-sõltuvad kinaasid (Cdk). Pagaripärmis kontrollib Cdk1 rakutsükli kulgemiseks vajalikke protsesse. Cdk-d vajavad aktiivsuseks tsükliini seondumist. On näidatud, et tsükliinid muudavad Cdk1 aktiivsust ja määravad substraatide valikut. Tsükliine sünteesitakse ja lagundatakse rakkudes kindlatel hetkedel, kusjuures erinevad tsükliinid ilmnevad rakus konkreetsetes järjekorras ja kontrollivad kindlaid rakutsükli protsesse. Tsükliinid Clb5 ja Clb6 on oma aminohappelise järjestuse poolest umbes 40% sarnased. Nad mõlemad ekspresseeritakse G1 faasi lõpus ja and vastutavad S faasi kulgemise ja DNA replikatsiooni eest. Kuigi erinevalt tsükliinist Clb5 ja

teistest B-tüüpi tsükliinidest, mis lagundatakse M faasis, langeb Clb6 valgu tase rakus juba S faasis. See viitab, et tsükliinil Clb6 on erinev degradatsiooni mehhanism võrreldes tsükliiniga Clb5. Käesoleva töö eesmärgiks oli uurida seda mehhanismi.

Võtmesõnad:

rakutsükkel, tsükliin, tsükliinsõltuv kinaas, seondumismotiivid, fosfo-degron, fosforüülimine, valkude degradatsioon

CERCS: P310, proteiinid, ensümolooia

TABLE OF CONTENTS

ABBREVIATIONS	6
INTRODUCTION	7
1 LITERATURE REVIEW	8
1.1 The cell cycle	8
1.2 Cdk1 regulation	9
1.3 SCF and APC mediated protein degradation.....	13
1.4 S phase cyclins Clb5 and Clb6	14
2 THE AIMS OF THE THESIS	15
3 EXPERIMENTAL PART	16
3.1 MATERIALS AND METHODS	16
3.1.1 Materials	16
3.1.2 PCR.....	20
3.1.3 Restriction/digestion.....	21
3.1.4 Ligation.....	22
3.1.5 Chemical bacterial transformation.....	22
3.1.6 Plasmid extraction	23
3.1.7 Lithium-Acetate mediated yeast transformation.....	23
3.1.8 Time-lapse microscopy.....	24
3.1.9 Protein Purification	25
3.1.10 Kinase assay.....	26
3.1.11 Western Blot	26
3.2 RESULTS AND DISCUSSION.....	29
3.2.1 Clb6 N-terminus does not have docking motif sequences specific to Clb5- Cdk1	30

3.2.2	Clb6-Cdk1 complex phosphorylates Clb6 N-terminus more efficiently than other Cyclin-Cdk1 complexes.	31
3.2.3	Clb6 N-terminus does not inhibit Cln2-Cdk1 or Clb5-Cdk1 complexes	32
3.2.4	Deletion of <i>clb5</i> results in prolonged presence of Clb6 in cells	33
3.2.5	Clb6-Cdk1 might phosphorylate itself <i>in trans</i> and trigger Clb6 degradation. 34	
SUMMARY		38
REFERENCES		40
NON-EXCLUSIVE LICENCE TO REPRODUCE THESIS AND MAKE THESIS PUBLIC		45

ABBREVIATIONS

aa – Amino acids

APC – Anaphase-promoting complex

ATP – Adenosine triphosphate

Cdk – Cyclin-dependent kinase

CSM – Complete supplement mixture D-box – Destruction box

DMSO – Dimethyl sulfoxide

HA tag – Human influenza hemagglutinin tag

His tag – Polyhistidine-tag

hp – Hydrophobic patch

hpm – Hydrophobic patch mutant

IPTG – Isopropyl β -D-1-thiogalactopyranoside

NLS – Nuclear localization signal

NLxxxL - Short linear Clb5-specific docking motif

SCF – Skp1-Cul-F-box

SDS – Sodium dodecyl sulfate

SDS-PAGE – Sodium dodecyl sulphate–polyacrylamide gel electrophoresis

SLiMs- Short linear motifs

SS-DNA – Salmon sperm single-stranded DNA

TE buffer – Tris-EDTA buffer

WT – Wild-type

YPD –Yeast extract, Peptone, Dextrose

INTRODUCTION

The cell cycle is a complex, tightly regulated, and timely controlled process. In yeast, it is divided into four phases (G1, S, G2, and M) and it is mainly regulated by the cyclin-dependent kinase Cdk1. Cdk1 activation requires binding to cyclins. There are 9 different cyclins that bind Cdk1 in yeast. They are expressed and degraded in a specific order and are responsible for different cell cycle events. G1 cyclins control the initiation of the cell cycle. S phase cyclins are responsible for S phase entry, progression, and efficient DNA replication. G2 and M phase cyclins are involved in mitotic events such as spindle morphogenesis and preventing mitotic exit and cytokinesis. Progression through S, G2 and M phases is controlled by six homologous B-type cyclins. Timely degradation of cyclins is important for correct progression through the cell cycle. Most B-type cyclins are degraded via anaphase-promoting complex (APC) mediated proteolysis in mitosis. APC and SCF complexes are two of the main ubiquitin ligases. They recognize specific degron motifs and polyubiquitinate target proteins. This leads to the degradation of the target proteins by the 26S proteasome.

Clb5 and Clb6 are the S phase cyclins that regulate DNA replication and other S phase processes. They share ca. 40% amino acid similarity and are expressed in the cell at the same time. However, Clb5 levels stay elevated until M phase, whereas Clb6 levels drop in the S phase. It has been shown that N-terminal truncations of Clb6 lead to its stabilization. Moreover, 3 phosphorylation sites (S6, T39, and S147) have been shown to be important for its timely degradation. Therefore, important regulatory elements could be in the intrinsically disordered N-terminus of Clb6.

In this work, we wanted to decipher the process of Clb6 degradation. For this, we created a set of Clb6 mutants with disrupted putative regulatory elements. We performed kinase assays to determine the cyclin-Cdk1 complex that phosphorylates the N-terminus of Clb6 and to investigate potential docking interactions between Clb5 and the N-terminus of Clb6. In addition, we tested potential inhibition of Cln2- and Clb5-Cdk1 by the N-terminus of Clb6. To investigate Clb6 levels *in vivo*, we performed western blot and time-lapse microscopy experiments.

1 LITERATURE REVIEW

1.1 The cell cycle

A cell's life period from one division to the next one is called the cell cycle. In *S. cerevisiae* cell cycle is divided into 4 distinct phases: G₁, S, G₂, and M (**Figure 1**). During the first phase of the cell cycle (G₁), cells grow and synthesize the required enzymes and nutrients required for the rest of the cycle. During the synthesis (S) phase, cells' DNA is replicated. In G₂ phase, which is known to be the shortest step in the cycle, cells continue their growth, and the newly replicated chromosomes are prepared for segregation. Cell cycle concludes when cells divide during mitosis (M phase). In case the conditions do not favor the transition to the S phase, cells may stay arrested in G₁ for a while or even enter G₀, also known as the non-dividing state (e.g., mating or unfavorable growth conditions) (Morgan, 2007).

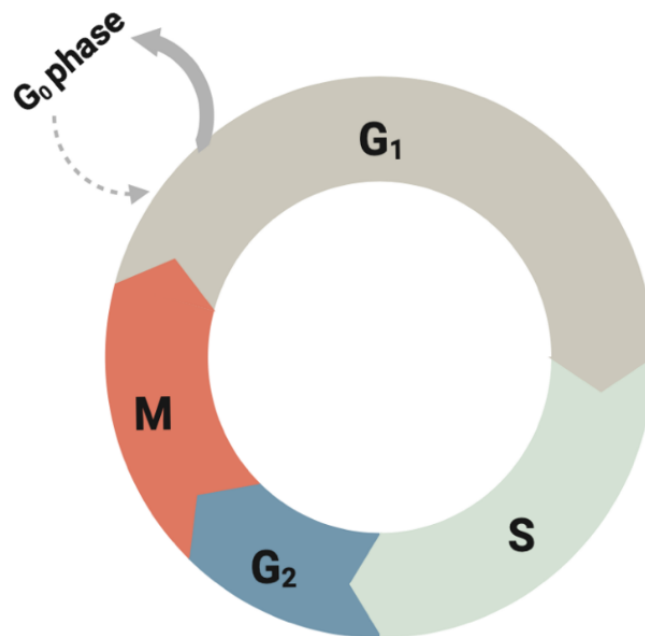


Figure 1. The cell cycle diagram. The cell cycle consists of four stages: G₁, S, G₂, and M. G₁ and G or in other words, Gap phases are control phases in which the cells get to grow and prepare for entry into the next phase. In case the environment is not favorable for division, cells could enter a prolonged state of no division or G₀ phase (Morgan, 2007).

The cell cycle is best understood in the budding yeast *S. cerevisiae* and is controlled by the regulatory network in cells that executes the events of the cell cycle. This regulatory network ensures the timely progression of the cell cycle as well as the events happening in a well-ordered manner by controlling a series of various biochemical events, causing progress through the checkpoints (Örd & Loog, 2019). There are three major checkpoints in the cell cycle. The first one happens at the G1/S transition, in which cells must choose whether to divide, mate, or enter G₀. The G1 checkpoint checks for cell size, nutrients, growth factors, and DNA integrity. The second checkpoint, or the G2 checkpoint, checks for DNA damage and DNA replication validity. The third is called the spindle checkpoint, it takes place in the metaphase, in which the cell checks for the correct attachment of chromosome to spindles at the metaphase plate. Progression through these checkpoints is mediated by Cyclin-dependent Kinase (Cdk) (Barnum & O’Connell, 2014).

Cyclin-dependent Kinases (Cdks) belong to a family of enzymes that catalyze the phosphorylation of proteins, the process through which a phosphoryl group transfers from an ATP molecule to a substrate protein (Morgan, 2007). *S. cerevisiae* is known to have six conserved Cdks: Cdk1(Cdc28), Pho85, Kin28, Ssn3, Ctk1, and lastly Bur. In yeast, Cdk1 executes hundreds of phosphorylation events, and it is the main regulator of the cell cycle ordering and progression (Enserink & Kolodner, 2010; Örd & Loog, 2019). The phosphorylation of the target proteins has various effects and may alter their stability, localization, activity, and interactions (Morgan, 2007; Örd & Loog, 2019). Cdk1 possesses several mechanisms to regulate its activity and substrate specificity, distinguish between early and late substrates, and ensure correct progression through the cell cycle.

1.2 Cdk1 regulation

Cdk1 is identified to be a serine/threonine proline-directed kinase. It catalyzes the phosphorylation of the full consensus motif Threonine/Serine-Proline-x- Lysine/Arginine (S/T-P-x-K/R), where “x” stands for any amino acid, and minimal consensus motif S/T-P (Örd & Loog, 2019).

Cdks require the attachment of the regulatory protein subunits known as cyclins to be catalytically active (Pines, 1995). Cyclin levels in the cell oscillate since they are periodically synthesized and degraded at specific points in the cell cycle. (Bloom & Cross, 2007; Jackson *et al.*, 2006; Richardson *et al.*, 1989) (**Figure 2**). *S. cerevisiae* expresses nine different cyclins that bind Cdk1. They are divided into groups based on their function and timing of

expression: G1 cyclin Cln3, G1/S cyclins Cln1, Cln2, S cyclins Clb5 and Clb6, G2 cyclins Clb3, Clb4, M cyclins Clb1, Clb2 (Bloom & Cross, 2007). Different Cyclin-Cdk1 complexes promote different events in the cell cycle (Loog & Morgan, 2005; Örd & Loog, 2019).

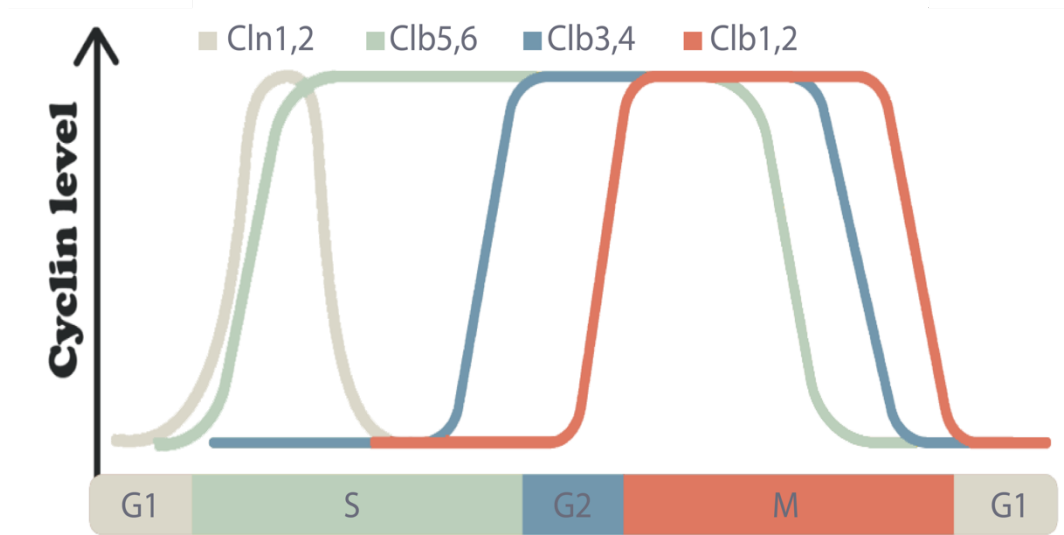


Figure 2. Cyclin expression profiles during different phases of the cell cycle. The scheme shows how all nine different cyclins expressed in *S. cerevisiae* oscillate throughout the cell cycle. Cln1,2 are G1/S cyclins taking part in the initiation of the cell cycle. S cyclins Clb5,6 contribute to DNA replication and Clb3 and Clb4 are G2 cyclins aiding entry into mitosis. Clb1 and Clb2 take part in mitotic events (Morgan, 2007).

The three *CLN* cyclins regulate entry into the cell cycle. The mutants lacking all three *CLN* genes cannot initiate the cycle and are arrested in G1. However, expression of one *CLN* gene is enough for initiation of the cell proliferation (Richardson *et al.*, 1989). Cln3 has a less oscillating expression profile, it is present during the entire cell cycle, and plays an important role in the transcription of the other two G1 Cyclins (Bloom & Cross, 2007; Jackson *et al.*, 2006).

B-type cyclins (Clb5 and Clb6) appear in the late G1 phase and are required for S phase entry, progression, and efficient DNA replication. Lastly, B-type cyclins Clb1-4 are involved in mitotic events such as spindle morphogenesis and preventing mitotic exit and cytokinesis (Bloom & Cross, 2007; Jackson *et al.*, 2006; Richardson *et al.*, 1989).

Cyclins are shown to target the Cyclin-Cdk complexes to specific substrates. Therefore, different cyclins lead to the phosphorylation of specific proteins during different cell cycle

phases and this cyclin specificity ensures an ordered progression through the cell cycle (Faustova *et al.*, 2021; Örd *et al.*, 2020).

Cdk1 intrinsic activity depends on the cyclin which is bound to it. The activity increases with progression through the cell cycle, meaning that G1 Cyclin-Cdk1 complexes are less active towards the model peptide (containing full consensus motif) compared to M phase Cyclin-Cdk1 complex (Kõivomägi *et al.*, 2011) (**Figure 3**).

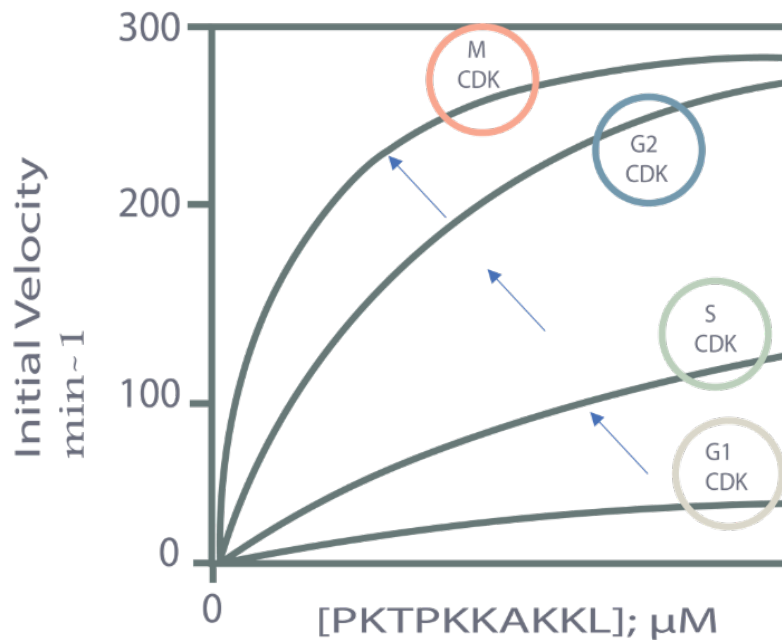


Figure 3. The activity of CDK complex increase along with the cell cycle progression. The Scheme shows how intrinsic Cdk1 activity depends on the cyclin bound to it. The Initial velocity was measured for a peptide containing a full consensus motif (Kõivomägi *et al.*, 2011).

Next, cyclins recognize and bind short linear motifs (SLiMs, also referred to as docking motifs) on the substrates, lowering the K_M of the substrates and promoting phosphorylation. For example, G1 cyclins recognize the LP motif (Bandyopadhyay *et al.*, 2020). S phase cyclins (Clb5-Cdk1) recognize NLxxxL (Faustova *et al.*, 2021), M cyclins recognize the LxF motif (Örd *et al.*, 2019), and B-type cyclins recognize the RxL motif (Loog & Morgan, 2005). Cyclins have a specific hydrophobic patch (*hp*) pocket that binds to these motifs (Brown *et al.*, 1999; Schulman *et al.*, 1998). Mutations in either *hp* pocket of the cyclin (usually referred to as *hpm*) lead to a decreased rate of phosphorylation (Faustova *et al.*, 2021; Örd *et al.*, 2019).

Recently, it was shown that phenylalanine at position 284 (F284) on the surface of the Clb5 recognizes and binds either NPF or DPF motifs in Cdk inhibitor proteins. The mutation of phenylalanine to alanine (F284A) eliminates this docking interaction (Prof. Mart Loog's laboratory unpublished data).

Another level of enzyme-substrate interaction is mediated via Cks1 phospho-docking. Cks1 is a phosphoadaptor protein that is a part of the Cyclin-Cdk complex. It is able to bind phosphorylated threonines but not serines. Furthermore, it promotes multisite phosphorylation by acting as an extension to the substrate-binding surface (Kõivomägi *et al.*, 2013). Moreover, the relative distance between docking and phosphorylation sites is important for catalyzing phosphorylation (Kõivomägi *et al.*, 2013). A summarized representation of these substrate Cdk complex interactions is presented in **Figure 4**.

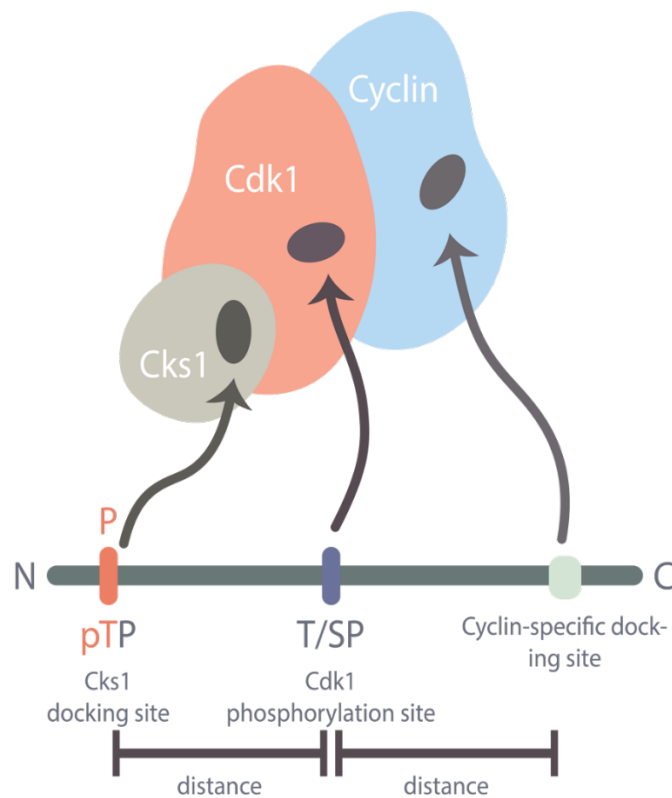


Figure 4. Main interactions between substrate proteins and the CDK complex. Schematic showing the major interactions between Cdk1 and substrate proteins. These interactions determine the phosphorylation rate and specificity (Örd & Loog, 2019).

All the aforementioned docking interactions may lead to up to a 100-fold increase in phosphorylation compared to the model peptide. Therefore, docking interactions allow less ac-

tive, early Cyclin-Cdk complexes to phosphorylate early substrates and prevent phosphorylation of the late substrates. The higher activity of the later Cyclin-Cdk complexes allows to keep early substrates in the phosphorylated state even without docking interactions and enables phosphorylation of the late substrates (Örd & Loog, 2019).

1.3 SCF and APC mediated protein degradation.

Progression through the cell cycle also depends on the timely degradation of specific proteins that are marked for degradation via polyubiquitination. SCF (Skp1/Cullin/F-box) or APC (anaphase-promoting complex) complexes are two of the main ubiquitin ligases (E3 Ub-ligases) that control protein degradation (Morgan, 2007).

Skp1, Cullin, and Rbx1/Roc1 are the three main components of the SCF complex. The complex works hand in hand with an adapter subunit known as the F-box protein, which functions as a direct substrate recruiter. The presence of posttranslational modifications, most notably glycosylation and phosphorylation, helps F-box proteins recognize their substrates (Ang & Harper, 2005; Feldman *et al.*, 1997). The Cdc4 protein in yeast is a known example of the F-box protein. Phosphorylated motifs in the substrate, known as phospho-degrons, engage directly with F-box proteins, providing a direct link with the ubiquitination machinery (Skowyra *et al.*, 1997).

One of the well-studied examples is phospho-dependent degradation in Sic1. Sic1 plays an important role in cell cycle control by preventing premature entry to the S phase via Clb5 inhibition. Sic1 is a disordered protein that contains regulatory N-terminus and inhibitory C-terminus (Kõivomägi *et al.*, 2011). The N-Terminus contains phospho-degrons that, if phosphorylated, send Sic1 for SCF mediated ubiquitination and subsequent degradation by the 26S proteasome (Kõivomägi *et al.*, 2011; Venta *et al.*, 2020; Verma *et al.*, 2001).

The APC-induced ubiquitin-dependent degradation of cell cycle proteins is a crucial process for cell division. APC is co-activated by distinct subunits: Cdc20 and Cdh1. Cdc20 and Cdh1 recognize specific motifs called D-box and KEN-box degrons on the target substrates. Classical D-box motif is RxxLxxI/VxN, and KEN-box motif is KENxxxN/D. Either both or any of the degrons are necessary for effective degradation of the target proteins. It is worth noting that APC^{Cdc20} prefers D-box degrons, while APC^{Cdh1} prefers KEN-box (Barford, 2011).

B-type cyclins are also marked for degradation via polyubiquitination by APC complex (Bäumer *et al.*, 2000; Shirayama *et al.*, 1999)

1.4 S phase cyclins Clb5 and Clb6

MBF transcription factor activates the expression of both Clb5 and Clb6 cyclins during the late G1 phase in *S. cerevisiae* cells. Both cyclins play an important role in S phase entry and progression (Jackson *et al.*, 2006; Schwob & Nasmyth, 1993). Clb5 and Clb6 have about 40% similarity in their amino acid sequence. Despite the similarity between the amino acid sequences, *clb5* and *clb6* mutants have shown multiple phenotypic differences in DNA replication and duplication of the spindle pole body (Jackson *et al.*, 2006b; Schwob & Nasmyth, 1993). Cells lacking Clb5 (*clb5* Δ) exhibit an extended S phase and significantly slowed DNA replication, moreover, firing of the late origins of replication was ineffective (Donaldson *et al.*, 1998). On the other hand, *CLB6* deletion (*clb6* Δ) did not affect the replication initiation of the late-firing origins (Donaldson *et al.*, 1998). Clb6 has been shown to phosphorylate the transcription factor Swi6 at serine 160 which directs the nuclear transportation of this transcription factor from the nucleus to the cytoplasm to curtail further G1 activity (Geymonat *et al.*, 2004; Haase *et al.*, 2001; Jackson *et al.*, 2006). However, it is worth noting that deletion of both genes causes delayed entry into the S phase (Schwob & Nasmyth, 1993). The observed phenotypic differences could be the outcome of different post-transcriptional regulations and protein functions (Jackson *et al.*, 2006).

Clb5 and Clb6 exhibit different stability profiles throughout the cell cycle. Levels of both Clb5 and Clb6 raise in the late G1. Clb5 levels are stable throughout the S phase and drop in the M phase when Clb5 gets destructed through the APC^{Cdc20} targeting. Clb6, on the other hand, is rapidly degraded at the G1/S border by the activity of the SCF^{Cdc4} complex (Jackson *et al.*, 2006; Morgan, 2007). Interestingly, there are also APC degrons, KEN box and D-box in the N-terminus of Clb6 and APC^{Cdh1} has been demonstrated to affect Clb6 degradation in the G1 phase (Wu *et al.*, 2016).

Clb6 rapid degradation in the S phase may be caused by phospho-dependent degradation. It has been shown that N-terminal truncations of Clb6 lead to its stabilization. Furthermore, three phosphorylation sites at positions 6, 39, and 147 (S6, T39, and S147) were shown to play a crucial role in Clb6 stability. Mutation of these phospho-sites to the non-phosphorylatable residue alanine (S6A, T39A, and S147A) led to hyper stabilization of Clb6. (Jackson *et al.*, 2006).

2 THE AIMS OF THE THESIS

Unlike other B-type cyclins that are degraded in the M phase, Clb6 levels decrease rapidly already in the S phase, which raises the question of its regulation mechanisms. It was previously shown that the N-terminal part of the Clb6 plays an important role in its oscillations. Moreover, three phosphorylation sites S6, T39, and S147 are crucial for its stability.

The aims of this thesis are:

- determining the Cyclin-Cdk1 complex that catalyzes the phosphorylation of the N-terminus of Clb6.
- determining linear motifs in the N-terminus of Clb6 that are important for its degradation.

3 EXPERIMENTAL PART

3.1 MATERIALS AND METHODS

3.1.1 Materials

Following materials and media were used for the experiments.

DNA cloning:

- a) TAE buffer: 40 mM Tris-acetate pH 8.3 and 1 mM EDTA
- b) 1% agarose TAE gel: 1 mM ethylenediaminetetraacetic acid (EDTA), 5 µl/l Atlas ClearSight DNA Stain (BioAtlas), 40 mM Tris-acetate pH 8.3 and 1% agarose;
- c) LB media: 5 g/l yeast extract (Formedium), 10 g/L NaCl (Chempur) and 10 g/l tryptone (Formedium)
- d) LB agar plates with ampicillin or kanamycin: LB media, 15 g/l bacto agar (Formedium), 100 µg/ml ampicillin (Sigma) or 100 µg/ml kanamycin (Sigma)
- e) LB agar plates with kanamycin and chloramphenicol: LB media, 15 g/l bacto agar (Formedium), 100 µg/ml kanamycin (Sigma) and 50 µg/ml chloramphenicol (Sigma).

Yeast transformation:

- a) YPD media: 20 g/l glucose (Oriola), 10 g/l yeast extract (Formedium) and 20 g/l peptone (Formedium)
- b) YPD plates: 20 g/l glucose (Oriola), 10 g/l yeast extract (Formedium), 20 g/l peptone (Formedium), 15 g/l bacto agar (Formedium)
- c) YPD/ClonNat plates: 20 g/l glucose (Oriola), 10 g/l yeast extract (Formedium), 20 g/l peptone (Formedium), 15 g/l bacto agar (Formedium), Nourseothricin (HKI, Jena, CAS#96736-11-7) (100 µg/ml)
- d) 1x TE buffer: 10 mM Tris hydrochloride (Tris-HCl) pH 8 and 1 mM EDTA
- e) PL1 buffer: 100 mM Lithium Acetate dissolved in 0.5 x TE buffer
- f) PL2 buffer: 40% Polyethylene glycol (PEG) 3350, 100 mM Lithium Acetate, 10 mM
- g) Tris-HCl pH 8, 1 mM EDTA
- h) SC-LEU glucose agar plates: 20 g/l glucose (Oriola), 20 g/l bacto agar (Formedium), 2 g/l SC-LEU powder (MP Biomedicals), 7 g/l yeast nitrogen base without amino acids (BD Biosciences).

Western Blotting:

- a) Urea lysis buffer: 20mM Tris pH=7.4, 8M Urea (Sigma), 2M Thiourea (Sigma), 4% CHAPS (Sigma), 1% DTT (Sigma), 50mM NaF, 89mM BGP, 1mM Na₃VC₄
- b) 6xSDS buffer: 0.375 M Tris-HCl pH 6.8, 0.6M DTT, 12% SDS (Sodium Dodecyl Sulphate), 60% Glycerol, 0.06% Bromophenol blue
- c) Semi-dry buffer: 25mM Tris-HCl, 192mM glycine, 0.1% SDS
- d) 1xTBS-T buffer: 20 mM Tris-HCl, 150 mM NaCl, 0.1%, Tween20 (Bio-Rad)
- e) Blocking solution: 5% fat-free milk powder, 1xTBS-T buffer
- f) Primary antibody solution: 3% fat-free milk powder, 1xTBS-T buffer, 1:500 anti-HA.11 antibody mouse IgG1 (clone 16B12, BioLegend Cat. No. 901501)
- g) Secondary antibody solution: 3% milk powder, 1xTBS-T buffer, 1:7500 HRP-conjugated anti-mouse IgG antibody (LabAS)

Kinase assay:

- a) 5x kinase buffer (5xKB): 250 mM Hepes-KOH (pH 7.4), 500 mM NaCl, 25 mM MgCl₂, 2.5 mM ATP
- b) SDS–polyacrylamide (SDS-PAGE) separating gel: 0.375 M Tris-HCl (pH 8.8), 12% acrylamide [29:1 acrylamide:bis-acrylamide], 0.1% SDS
- c) SDS-PAGE stacking gel: 0.125 M Tris-HCl (pH 6.8), 5% acrylamide [29:1acrylamide:bis-acrylamide], 0.1% SDS)
- d) SDS-PAGE running buffer: 25 mM Tris, 192 mM glycine, 0.1% SDS
- e) Coomassie R250 staining solution (0,1 % Coomassie Blue R250 (w/w), 30 % methanol, 5 % acetic acid)
- f) Destain solution (30 % methanol, 5 % acetic acid)

Protein purification:

- a) Lysis buffer: 25 mM Hepes-KOH pH 7.4, 300 mM NaCl, 10% glycerol
- b) Protease inhibitors: 1 mM phenylmethylsulphonyl fluoride (PMSF), 1 µg/ml pepstatin A, 1 µg/ml aprotinin, 1 µg/ml DnaseI
- c) Elution buffer: 25 mM Hepes-KOH pH 7.4, 300 mM NaCl, 10% glycerol, 200mM imidazole

Time lapse microscopy:

- a) Synthetic complete media (CSM) with 2% glucose: 20 g/l peptone (Formedium), 10g/l CSM (Formedium), 20 g/l glucose (Oriola).
- b) 1.5% SC/glucose-agarose gel pad: 20 g/l peptone (Formedium), 10 g/l CSM (Formedium), 20 g/l glucose (Oriola), 1.5% NuSieve GTG agarose (Lonza).

Table 1. List of yeast strains used in the study. The list contains the name of the strain, information on the background strain and a brief description of the strain.

Strain	Background strain	Description
AM1	RV298	<i>MATa RHO+</i> , <i>Whi5::mCherry-SpHis5</i> , <i>ADE2+</i> , <i>bar1::HisG TRP1::PACT1(-1-520)-LexA-ER-haB112-TCYC1</i>
AM2	AM1	<i>LEU2::PLEXA-clb6(S6A S9A)-mCitrine-NLS-TCYC1</i>
AM3	AM1	<i>LEU2::PLEXA-clb6(T39A)-mCitrine-NLS-TCYC1</i>
AM4	AM1	<i>LEU2::PLEXA-clb6(S9A KEN-box D-box)-mCitrine-NLS-TCYC1</i>
AM5	AM1	<i>LEU2::PLEXA-CLB6-mCitrine-NLS-TCYC1</i>
AM6	AM1	<i>LEU2::PLEXA-clb6(KEN-box D-box)-mCitrine-NLS-TCYC1</i>
AM9	AM1	<i>LEU2::PLEXA-clb6(S6A S9A KEN-box D-box)-mCitrine-NLS-TCYC1</i>
AM10	AM1	<i>LEU2::PLEXA-clb6(1-100 KEN-box D-box)-mCitrine-NLS-TCYC1</i>
AM11	AM1	<i>LEU2::PLEXA-clb6(1-100 S6A S9A)-mCitrine-NLS-TCYC1</i>
AM12	AM1	<i>LEU2::PLEXA-clb6(1-100 WT)-mCitrine-NLS-TCYC1</i>
AM13	AM1	<i>LEU2::PLEXA-clb6(1-100 S9A KEN-box D-box)-mCitrine-NLS-TCYC1</i>
AM14	AM1	<i>LEU2::PLEXA-clb6(1-100 T39A)-mCitrine-NLS-TCYC1</i>
AM15	AM1	<i>LEU2::PLEXA-clb6(1-100 S6A S9A KEN-box D-box)-mCitrine-NLS-TCYC1</i>
AM16	AM1	<i>LEU2::PLEXA-clb6(1-120 WT)-mCitrine-NLS-TCYC1</i>
AM17	AM1	<i>LEU2::PLEXA-clb6(1-120 S6A S9A KEN-box D-box)-mCitrine-NLS-TCYC1</i>
AM18	AM1	<i>LEU2::PLEXA-clb6(1-120 S9A KEN-box D-box)-mCitrine-NLS-TCYC1</i>

AM19	AM1	<i>LEU2::PLEXA-clb6(1-120 KEN-box D-box)-mCitrine-NLS-TCYC1</i>
AM20	AM1	<i>LEU2::PLEXA-clb6(1-120 T39A)-mCitrine-NLS-TCYC1</i>
AM21	AM1	<i>LEU2::PLEXA-clb6(1-120 S6A S9A)-mCitrine-NLS-TCYC1</i>
AM31	RV298	<i>MATa RHO+, Whi5::mCherry-SpHis5, ADE2+, bar1::HisG CLB6:6xHA-pAgTEF-nat-tScADH1</i>
AM32	MO668	<i>clb5Δ::URA3, Whi5::mCherry-SpHis3 CLB6:6xHA-pAgTEF-nat-tScADH1</i>
AM33	MO367	<i>clb5Δ::CLB2 swe1Δ::uraX, Whi5::mCherry-SpHis5 CLB6:6xHA-pAgTEF-nat-tScADH1</i>

Table 2. Plasmids used in this study. Each row in the table contains the name of the plasmid, plasmid content, the backbone vector, and the source.

Plasmid	Backbone	Description	Source
pYM17		PCR template for C-terminal 6xHA tag: marker pAg-TEF-nat-tScADH1, selectable phenotype: clonNAT resistance.	(Janke <i>et al.</i> , 2004)
pRG205MX		Integrative vector backbone, LEU2MX selection marker.	(Gnügge <i>et al.</i> , 2016)
pAM0033	pRG205MX	<i>PLEXA-mCitrine-NLS-TCYC1</i>	This Study
pAM0059	pRG205MX	<i>PLEXA-CLB6-mCitrine-NLS-TCYC1</i>	This Study
pAM0060	pRG205MX	<i>PLEXA-clb6(KEN-box D-box)-mCitrine-NLS-TCYC1</i>	This Study
pAM0061	pRG205MX	<i>PLEXA-clb6(S6A S9A)-mCitrine-NLS-TCYC1</i>	This Study
pAM0063	pRG205MX	<i>PLEXA-clb6(T39A)-mCitrine-NLS-TCYC1</i>	This Study
pAM0067	pRG205MX	<i>PLEXA-clb6(S6A S9A KEN-box D-box)-mCitrine-NLS-TCYC1</i>	This Study
pAM0073	pRG205MX	<i>PLEXA-clb6(1-100 KEN-box D-box)-mCitrine-NLS-TCYC1</i>	This Study
pAM0074	pRG205MX	<i>PLEXA-clb6(1-100 S6A S9A)-mCitrine-NLS-TCYC1</i>	This Study
pAM0075	pRG205MX	<i>PLEXA-clb6(1-100 T39A)-mCitrine-NLS-TCYC1</i>	This Study
pAM0076	pRG205MX	<i>PLEXA-clb6(1-100 S6A S9A KEN-box D-box)-mCitrine-NLS-TCYC1</i>	This Study
pAM0077	pRG205MX	<i>PLEXA-clb6(1-100 S9A KEN-box D-box)-mCitrine-NLS-TCYC1</i>	This Study
pAM0078	pRG205MX	<i>PLEXA-clb6(1-100)-mCitrine-NLS-TCYC1</i>	This Study
pAM0079	pRG205MX	<i>PLEXA-clb6(1-120)-mCitrine-NLS-TCYC1</i>	This Study
pAM0080	pRG205MX	<i>PLEXA-clb6(1-120 KEN-box D-box)-mCitrine-NLS-TCYC1</i>	This Study
pAM0081	pRG205MX	<i>PLEXA-clb6(1-120 T39A)-mCitrine-NLS-TCYC1</i>	This Study

pAM0082	pRG205MX	<i>PLEXA-clb6(1-120 S6A S9A KEN-box D-box)-mCitrine-NLS-TCYC1</i>	This Study
pAM0083	pRG205MX	<i>PLEXA-clb6(1-120 S9A KEN-box D-box)-mCitrine-NLS-TCYC1</i>	This Study
pAM0084	pRG205MX	<i>PLEXA-clb6(1-120 S6A S9A)-mCitrine-NLS-TCYC1</i>	This Study
pAM0047	pET28a	<i>clb6(1-120)-GB1</i>	This Study
pAM0051	pET28a	<i>clb6(1-120 S6A S9A)-GB1</i>	This Study
pAM0071	pET28a	<i>clb6(1-120 S9A T39)-GB1</i>	This Study
pAM0072	pET28a	<i>clb6(1-120 S6A T39)-GB1</i>	This Study

3.1.2 PCR

All *clb6* variants used in this work were obtained using digestion/ligation method. *clb6* variants were PCR amplified from *S. cerevisiae* w303 genomic DNA using Thermo Scientific Phusion High-Fidelity DNA Polymerase. The PCR reaction mix final volume was 50 μ l and the exact components are presented in **Table 3**. The three-step PCR program used for the amplification of *clb6* variants is shown in **Table 4**. Annealing temperature and DNA extension times were estimated separately for every set of primers.

Table 3. Three-step PCR mixture.

Component	μ l
DNA Template (15-50 ng)	1
5x Phusion HF Buffer (Thermo Fisher Scientific)	10
dNTPs (10 mM)	0.5
Phusion High Fidelity DNA Polymerase (Thermo Fisher Scientific)	0.5
Primer 1 (10 μ M)	2.5
Primer 2 (10 μ M)	2.5
Milli-Q H ₂ O	33

Table 4. Three-step PCR program.

Cycle step	Temperature (°C)	Time (s)	Number of Cycles
Initial Denaturation	98	300	1
Denaturation	98	20	30
Annealing	56-63	20	
Extension	72	30 s/kb	
Final extension	72	300	1
Hold	15	∞	1

After the completion of the PCR reactions, the mixture was stained with 6x Orange DNA Loading Dye (Thermo Fisher Scientific catalog number R0631) and consecutively loaded on to 1% or 2% Agarose gel (depending on the size of the fragment). DNA gel electrophoresis was performed in 1x TAE buffer together with ZipRuler DNA Ladder 1 or 2. The DNA products were observed under UV light, the right band was cut out from the gel after length estimations using ZipRuler DNA Ladder 1 or 2. Afterwards, the excised fragment was purified by FavorPrep GEL/PCR Purification Kit (Favorgen) according to the manufacturer's protocol.

3.1.3 Restriction/digestion

For the integration of the DNA fragment into the backbone vector, around 100 ng of PCR product and 1.5 µg of vector backbone was digested using FastDigest™ restriction enzymes. EcoRI and HindIII or NcoI and SacI FastDigest™ enzymes were used to clone *clb6* variants into pRG205MX or pET28a derived vectors, respectively. The restriction digestion reaction mixture is shown in **Table 5**.

Digestions were carried out at 37°C for 30 minutes. Afterwards, Fast Digest™ enzymes in PCR products reaction mixtures were heat-inactivated at 80°C for 10 minutes. Restricted vector backbones were stained with 6x Orange DNA Loading Dye (Thermo Fisher Scientific catalog number R0631) and loaded on 1% agarose gels. Afterwards, the DNA gel electrophoresis was performed. DNA bands of the correct size were cut out from agarose gel and DNA was extracted with FavorPrep GEL/PCR Purification Kit (Favorgen) according to the manufacturer's protocol.

Table 5. Restriction/digestion reaction mixture.

Component	μl
DNA (ca. 100 ng or 1.5 μg)	x
10x FastDigest™ Green buffer	2
FastDigest™ restriction enzyme A	0.5
FastDigest™ restriction enzyme B	0.5
Milli-Q H ₂ O	up to 20

3.1.4 Ligation

The last step in creating the recombinant plasmid prior to transforming them into competent cells was to ligate the linearized vector with the restricted insert. 1:3 vector to insert molar ratio was used. The ligation mixture is shown in **Table 6**. The ligation reaction was resuspended and incubated at 16°C for 2 to 24 hours.

Table 6. Ligation reaction mixture

Component	μl
Linearized vector (20-50 ng)	x
Linearized insert	2-3
10x ligation buffer (Thermo Fisher Scientific)	1
T4 DNA ligase (Thermo Fisher Scientific)	0.5
Milli-Q H ₂ O	up to 10

3.1.5 Chemical bacterial transformation

E. coli NEB Turbo competent cells were used to amplify ligated plasmid. *E. coli* NEB Turbo chemically competent cells were taken out of -80 °C and thawed on ice for approximately 10 minutes. 2-3 μl of the ligation mix was added to 50 μl of the competent cells, resuspended, and consecutively incubated on ice for 30 minutes. The mixture is then heat-shocked for 30 seconds at 42 °C, followed by 5 minutes of cooling down on ice. Subsequently, 500 μl of LB media was added to the mixture and incubated for 60 minutes at 37 °C in a 220 rpm shaker. Lastly, the cells were collected by centrifugation for 60 seconds at 6000 rpm, excessive LB media was removed, cells resuspended in the remaining (ca. 100 μl) LB media, plated on an LB plate containing the corresponding antibiotic, and incubated for 12-16 hours at 37 °C.

3.1.6 Plasmid extraction

2-3 colonies were taken from the bacterial transformation plates and grown in 4-5 ml of LB media containing the corresponding antibiotic (Ampicillin, Kanamycin). The glass tubes containing the growth media, antibiotic, and the single colony were then incubated in a 37°C shaker for 8-16 hours. Afterwards, plasmid DNA from the cells was isolated using FavorPrep Plasmid DNA Extraction Mini Kit (Favorgen) using the manufacturer's protocol. Quantity of the purified plasmid DNA was assessed with Thermo Fisher's NanoDrop 1000 Spectrophotometer. To make sure of the presence of the inserted fragment, the purified plasmid was restricted with the FastDigest™ enzymes that were used for the initial restriction digestion. Restriction digestion was further followed by gel electrophoresis of the restricted plasmid, the result observed under UV light. The correct plasmids were sent to Sanger sequencing to verify the results. Sanger sequencing was performed in the Institute of Genomics Core Facility.

3.1.7 Lithium-Acetate mediated yeast transformation

After the correctness of plasmids was verified with Sanger sequencing, *S. cerevisiae* cells were transformed with linearized integrative plasmid. In this work, linearized plasmids containing *clb6* variants fused to mCitrine and NLS under the control of *LexA* inducible promoter were integrated into *LEU2* locus. Plasmids were linearized with *SgsI* FastDigest™ enzyme. A day prior to the transformation, the yeast cells were streaked onto a fresh YPD plate and incubated in a 30°C incubator for 12-16 hours. On the following day, after the culture appeared on the plate, a small tip of an inoculation stick was covered with a sufficient amount of cells and the cells were then transferred to a flask containing 50 ml of YPD media. The culture is then incubated at 30°C with constant shaking until the OD_{600} reached a range of 0.6-0.8. Subsequently, cells were collected by centrifugation for 1 min at 3100 rpm. The supernatant was then removed and the pellet was resuspended in 1 mL of sterile buffer PL1 (100 mM lithium acetate in 0.5 x TE (5 mM Tris-HCl (pH 8), 0.5 mM EDTA) followed by another round of centrifugation for 1 min at 3600 rpm. The supernatant was removed once more, and the cells were again resuspended in two times the cell volume of PL1. The mixture was then incubated for 10 minutes at room temperature. In the meantime, salmon sperm DNA was boiled for 10 minutes at 100°C and afterwards cooled down on ice. Following this step, 100 µl of the competent yeast cells were mixed in a 1.5 µl Eppendorf tube with the 1-2 µg of linearized plasmid (integrative plasmid) and 10 µl of SS-DNA. 700 µl sterile buffer

PL2 (40% PEG 3350, 100 mM lithium acetate, 10 mM Tris-HCl (pH 8), 1 mM EDTA), and 48 μ l of DMSO were added to the same tube, resuspended gently and incubated at 42°C for 40 minutes. After incubation, the tubes were cooled down on ice for 2 minutes and centrifuged at 6000 rpm for 30 seconds. Supernatant was removed, cells were resuspended 1ml of 1x TE buffer and centrifuged for 1 minute at 3200 rpm. Supernatant was removed again; cells were resuspended in 200 μ l of 1x TE buffer and plated on a plate containing the correct selection media. Transformed yeast cells were incubated for 2-4 days at 30°C.

3.1.8 Time-lapse microscopy

Time-lapse microscopy was performed to measure and observe the levels of mCitrine fluorescence indicating the levels of clb6 during different stages of the cell cycle. By observing real-time changes in the Citrine levels, the expression or degradation of our protein of interest was indicated. Whi5 protein tagged with mCherry was used for cell cycle phase reference.

Before the experiment, yeast cells containing the integrated plasmid were incubated in 3 ml CSM 2% glucose media to the optical density of 0.3 to 0.6. 0.5 μ l of cells was then pipetted onto 24x50x0.08 mm micro cover glass and covered with CSM agar patches. For Clb6 induction, CSM agar patches with 500 nM β -Estradiol were used. Microscopy was carried out using the Zeiss observer Z1 microscope with automated stand, AxioCam 506 mono-camera, 63x/1.4NA oil immersion objective, temperature control and definite focus. During the experiments, the cells were kept at 30°C constant temperature.

12-16 of selected positions were photographed every 3 minutes for 8 hours during every experiment. 2-3 positions for every strain were selected. The images of phase-contrast, Clb6-mCitrine, Whi5-mCherry were taken every 3 minutes. The setup of the microscope is shown in the **Table 7**. After the experiment, images of all three channels were exported in JPG format, and the results were analyzed with MATLAB using scripts modifications of Doncic *et al.*, 2013. For graphical representation, cells were synchronized at 50% nuclear exit of Whi5.

Table 7. Zeiss observer Z1 setup for time-lapse microscopy.

	Phase contrast	Clb6-mCitrine	Whi5-mCherry
Reflector	72 HE CFP/YFP/DsRed	46 HE Yellow Fluoresc. Prot	72 HE CFP/YFP/DsRed
Light source	TL Halogen Lamp	LED-Module 505nm	LED-Module 567nm
Light source in- tensity	4.61 Volt	25%	25%
Excitation wavelength		524	587
Emission Wave- length		536	610
Exposure time	25 ms	250 ms	750 ms

3.1.9 Protein Purification

The immobilized metal affinity chromatography (IMAC) technique was used to purify proteins from the recombinant plasmids of interest. The C-terminally 6xHis affinity tagged proteins expressed in BL21(DE3) cells were attracted to the cobalt ions on the IMAC column and later eluted using 200 mM imidazole.

Selected colonies were put to grow in 200 ml LB media at 37°C to OD 0.6 and afterwards, the expression was induced with 1 mM Isopropyl β -D-1-thiogalactopyranoside (IPTG) for 3 hours. The cultures were then centrifuged at 5000 RPM for 10 minutes. The pellets were resuspended in 6 ml lysis buffer (25mM HEPES-KOH pH 7.4, 300 mM NaCl, 10% glycerol) plus 1 mg/ml lysozyme and protease inhibitors (1 mM phenylmethylsulphonyl fluoride (PMSF), 1 μ g/ml pepstatin A, 1 μ g/ml aprotinin, 1 μ g/ml DnaseI;). Cells were then transferred to 4 °C for 30 minutes to end-over-end rotator. This was followed by three times 20 seconds sonication (medium rod, 40-50% power). Cells were incubated on ice for 1 minute between sonication rounds. Following sonication, the lysates were centrifuged at 14800 RPM for 20 minutes at 4°C. In the meantime, column containing 100 μ l of the Chelating Sepharose (GE Healthcare) were washed with 1ml H₂O, then with 200 μ l of 200 mM CoCl₂, and followed by equilibration of the column with 10x column volumes (CV) of the Lysis buffer. After completion of centrifugation, the supernatants were loaded on the columns to flow through. Columns were then washed 2 times with 10x CV of lysis buffer and further with 10x CV ml lysis buffer supplemented with 50 mM imidazole to eliminate unspecific

binding of proteins to the column. Lastly, proteins were eluted 3 times with 1x CV of elution buffer (25 mM Hepes-KOH pH 7.4, 300 mM NaCl, 10% glycerol, 200mM imidazole). After purification, SDS polyacrylamide gel electrophoresis (SDS-PAGE) was used to check for the purity and concentration of the samples. The concentration of the samples was estimated using BSA standard curve. Elutions were frozen in liquid nitrogen and stored at -80°C before the kinase assays.

3.1.10 Kinase assay

Purified Clb6 (1-120 aa) variants were used as either substrates or inhibitors the phosphorylation reactions. The kinases used in this study were, Cln2-Cdk1, Clb5-Cdk1, Clb2-Cdk1 and Clb6-Cdk1 complexes. H1 and Sic1(1-215) were used as the control substrate. In case of the Kinase inhibition assay, different concentrations of Clb6(1-120) were used to inhibit either Cln2-Cdk1 or Clb5-Cdk1; in these reactions, Sic1(1-215) and H1 were used as substrates.

The phosphorylation reactions were done at room temperature in a buffer containing 50 mM Hepes-KOH with pH 7.4, 150 mM NaCl, 5 mM MgCl₂, 0.2 mg/ml BSA, 500 nM Cks1, and 500 μM ATP [(with added [γ -³²P]-ATP (Hartmann Analytic)]. The concentration of kinase complexes was approximately 0.2 nM, and substrate proteins were around 1 μM. Two time points (7 and 14 minutes) were collected, and the phosphorylation reaction was stopped by mixing the reaction mixture aliquot with an equal amount of the 2xSDS. SDS-PAGE was performed to separate proteins on the polyacrylamide gel and stained with Coomassie R250 staining solution to visualize proteins.

Amersham Typhoon 5 biomolecular Imager (GE Healthcare Life Sciences) was used to detect γ -³²P phosphorylation signals. The quantification of signals was done using ImageQuant TL (Amersham Biosciences), and Microsoft Excel was used for data analysis.

3.1.11 Western Blot

Western Blot was carried out using three different yeast *S. cerevisiae* strains (AM31, AM32, AM33). 50 ml of the yeast cultures were grown in a 30°C shaker until they reached OD 0.4 - 0.6, then cells were arrested in G1 phase with 10 ng/μl of α -factor for 2 hours. After the release from the arrest (3 times wash with 20 ml YPD), synchronized cell cultures went through the cell cycle and 3 ml samples of every strain were collected at time points 0, 10, 15, 20, 30, 35, 40, 50, 60, 75 minutes covering the entire *S. cerevisiae*'s cell cycle. To collect

cells, 3 ml of cultures were transferred to the 15 ml tube, centrifuged at 4000 rpm for 1 min, supernatant removed, and the cells frozen in the liquid nitrogen.

The cells were lysed with 200 μ l of urea lysis buffer. 1.5 ml tubes containing Silibeads were then prepared for the lysate to be added. The cells were then broken using the homogenizer (FastPrep -24, M.P Biomedicals) at 4 m/s for 40 seconds and subsequently centrifuged at the maximum speed of 13400 rpm for 10 minutes. Bradford assay was carried out to make sure all samples would have the same amount of total protein. Samples were then added to 1.5 ml Eppendorf tubes containing 6-12 μ l 2xSDS buffer. The samples were then heated in the incubator for 5 minutes at 72°C and loaded on a conventional SDS-PAGE (Sodium Dodecyl Sulphate - Polyacrylamide Gel Electrophoresis) gel, electrophoresis went on for 1 hour at 15mA per gel. Following electrophoresis gels, nitrocellulose membrane (Amersham, Germany) and filter papers (Blotting-Papier MN 827 B, Macherey-Nagel, Germany) were soaked in semi-dry transfer buffer for 15 minutes. For transferring, the sandwich was assembled by laying two filter papers on the anode of the power Blot Cassette, then the membrane and gel on the membrane, and finally two layers of filter paper on the gel. The transfer was done using the Fast Blotter (Thermo Scientific) and running the Standard semi-dry transfer Program for 1 hour. After the transfer was done, the membrane was placed in the Blocking solution (5% fat-free milk powder in TBS-T) for 1 hour at room temperature with gentle agitation or overnight at 4°C with 0.03% azide added to the blocking solution. Following blocking, the membrane was washed once with 1xTBS-T buffer and then transferred to the primary antibody solution (1/500 dilution in 3% milk TBS-T with 0.03% azide). The membrane was then washed with TBS-T 3 times with intense shaking each time for 15 minutes. HRP-conjugated secondary antibody (20 ml per gel, 3% milk TBS-T WITH 1/7500 dilution of the antibody) incubation took place for 30 minutes with gentle agitation. this step was followed by 3 times washing with TBS-T each time for 15 minutes with intense shaking. To visualize the protein bands on X-ray film, the membrane was covered with 600 μ l of the chemiluminescent (SuperSignalTM West Femto PLUS /Thermo Scientific) substrate with a 1:1 ratio of the two solutions and then covered entirely between two plastic wraps. The film (AGFA Medical X-Ray film blue, Belgium) was then put into a cassette containing the membrane for exposure to take place. To develop the film, it was dipped into the G150 developer (AGFA) for 30 seconds, dried for 5 seconds, dipped into water for 10 seconds, and finally dipped into the G354 fixer (AGFA) for 20 seconds and finally washed with water under the sink.

The dried film was then marked with the bands of the PageRuler™ Prestained protein Ladder.

3.2 RESULTS AND DISCUSSION

B-type cyclins Clb5 and Clb6 appear in the late G1 phase and are required for S phase entry and progression. Although Clb6 and Clb5 have similarities in amino acid sequence and transcriptional regulation, Clb6 gets rapidly degraded in the S phase while Clb5 levels remain stable until the M phase. Previous studies have shown that the N-terminal part of Clb6 plays an important role in its degradation, and alanine mutations at three phosphorylation sites at positions 6, 39, and 147 (S6, T39, S147) lead to hyper stabilization of Clb6 (Jackson *et al.*, 2006). It has been suggested that the degradation of Clb6 in the S phase might indicate the presence of phospho-degron(s) in the N-terminus of the protein. This degron(s) may be recognized by the SCF complex. IPSPIS amino acid sequence at positions 4-9 of the Clb6 N-terminus resembles Cdc4 phospho-degron consensus I/L/P-L/P-pS/pT-x-x-pS/pT (Faustova *et al.*, 2021). Clb6 N-terminus also has D-box at positions 64-72 (RGKLQRDST) and KEN box (positions 23-25) motifs, as well as potential Clb5 docking motif DPF at positions 113-115. Although some regulatory elements in the Clb6 amino acid sequence have been identified, the regulation of the Clb6 degradation is still unclear.

In this work, we wanted to decipher the process of Clb6 degradation. For doing so, a set of Clb6 mutants with disrupted putative regulatory elements was created. The annotated Clb6 N-terminus is shown in **Figure 5**.



Figure 5. Schematic representation of the N-terminal part of Clb6. Phosphorylation sites (S6, S9, T39), APC degron motifs (KEN-box and D-box), and putative Cdk1 docking motif (DPF) are depicted.

Kinase assays were performed to determine the Cyclin-Cdk1 complex that phosphorylates the N-terminus of Clb6 and furthermore, investigate potential docking interactions between Clb5 and the N-terminus of Clb6. In addition, the potential inhibition of Cln2- and Clb5-Cdk1 by Clb6 N-terminus was tested. To investigate Clb6 levels *in vivo*, western blot and time-lapse microscopy experiments were performed.

3.2.1 Clb6 N-terminus does not have docking motif sequences specific to Clb5-Cdk1

Amino acid sequence analysis indicates that Clb6 N-terminus possesses a potential Clb5 docking motif, DPF, at positions 113-115. To check for the presence of specific docking interactions between Clb5-Cdk1 and Clb6(1-120), different versions of Clb5 were used: wild-type (WT) Clb5, Clb5 with mutated hydrophobic patch pocket (Clb5_{hpm}), and Clb5 with alanine mutation at position 284 (Clb5_{F284A}). Mutations in the hydrophobic patch pocket lead to the loss of Clb5 ability to bind docking motifs on the substrates. F284 was shown to facilitate the binding of Clb5 to the N/D-P-F motif on substrates and the mutation of this phenylalanine to alanine eliminates this interaction. Kinase assays were performed with Clb6(1-120) WT as the substrate at the final concentration of ca. 1 μ M.

Kinase assay results indicate that there are no specific docking interactions between Clb5 and Clb6(1-120) (Figure 6). Phosphorylation of Clb6(1-120) by both Clb5- and Clb5_{hpm}-Cdk1 is similarly low. The phosphorylation signal observed in case of the Clb5_{F284A} is due to the higher amount of Clb5_{F284A} used for the assay, as it is seen on the H1 control lane. Therefore, DPF motif of Clb6 is probably non-functional and does not affect phosphorylation.

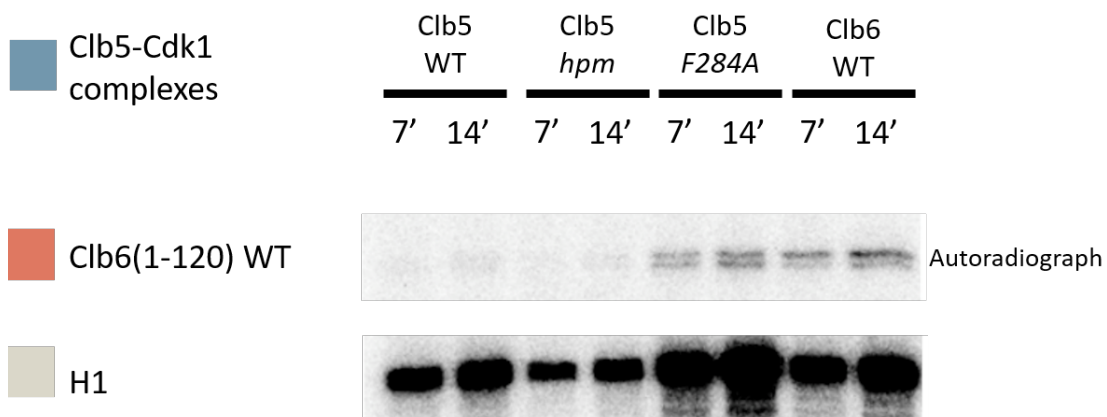


Figure 6. Phosphorylation of Clb6(1-120) by different versions of Clb5-Cdk1. Aliquots of two timepoints at 7 and 14 minutes were collected. The autoradiographs are shown. The relative activity of different Clb5-Cdk1 complexes could be estimated from the histone H1 autoradiograph.

3.2.2 Clb6-Cdk1 complex phosphorylates Clb6 N-terminus more efficiently than other Cyclin-Cdk1 complexes.

Kinase assay experiments were carried out to study different cyclins specificity towards Clb6(1-120). Variants of either wild-type N-terminus Clb6 or mutants with only one phosphorylation site (S6, S9, or T39) were created. All these Clb6 variants were used as substrates for kinase assays with the final concentration of 1 μ M. Histone H1 was used as the control substrate.

The results indicate that Clb6-Cdk1 complex phosphorylates Clb6(1-120) more efficiently compared to Cln2-, Clb5-, Clb2-Cdk1 (**Figure 7**). It might suggest that Clb6-Cdk1 is capable of *in trans* autophosphorylation of Clb6, which might lead to subsequent degradation. However, this hypothesis needs to be tested further.

Weak phosphorylation was observed in case of Clb2-Cdk1 and was almost absent in the case of Cln2- and Clb5-Cdk1 complexes. Clb6 mutant bearing only S6 phosphorylation site showed a higher level of phosphorylation compared to WT. This may be explained by pipetting error or a concentration difference between two substrates.

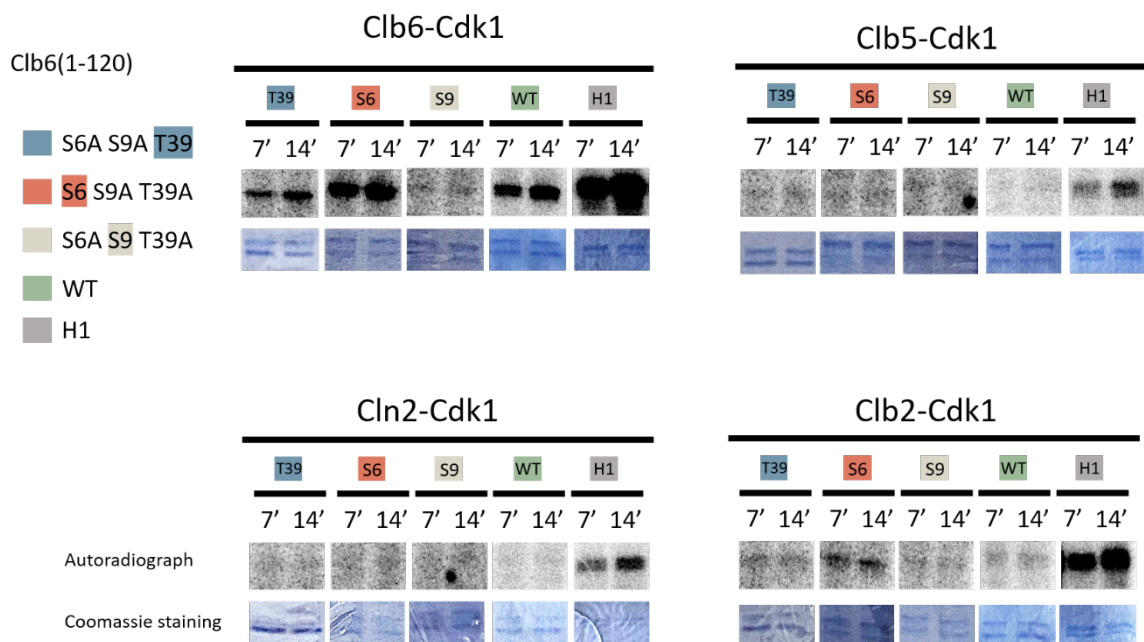


Figure 7. Phosphorylation kinase assay of Clb6(1-120) mutants by Clb6-, Clb5-, Cln2- and Clb2-Cdk1. Aliquots of two timepoints at 7 and 14 minutes were collected. The autoradiographs and corresponding images of the stained polyacrylamide gels are presented.

3.2.3 Clb6 N-terminus does not inhibit Cln2-Cdk1 or Clb5-Cdk1 complexes

The observed lack of Clb6(1-120) phosphorylation by Cln2- and Clb5-Cdk1 raised the question of whether the N-terminus of Clb6 may inhibit the above-mentioned Cyclin-Cdk1 complexes. To test this assumption, inhibitory kinase assays were performed. Different concentrations of Clb6(1-120) were added to the reaction mixture as the inhibitor. As control substrates, the non-inhibitory version of Sic1 (Sic1 Δ C), containing both consensus phosphorylation sites and cyclin docking motifs, and H1 which lacks docking motifs and only has a consensus phosphorylation site, were used. The results indicate that Clb6(1-120) does not inhibit the Cln2- and Clb5-Cdk1, since the presence of Clb6(1-120) does not affect the rate of substrates' phosphorylation (**Figure 8, A and B**).

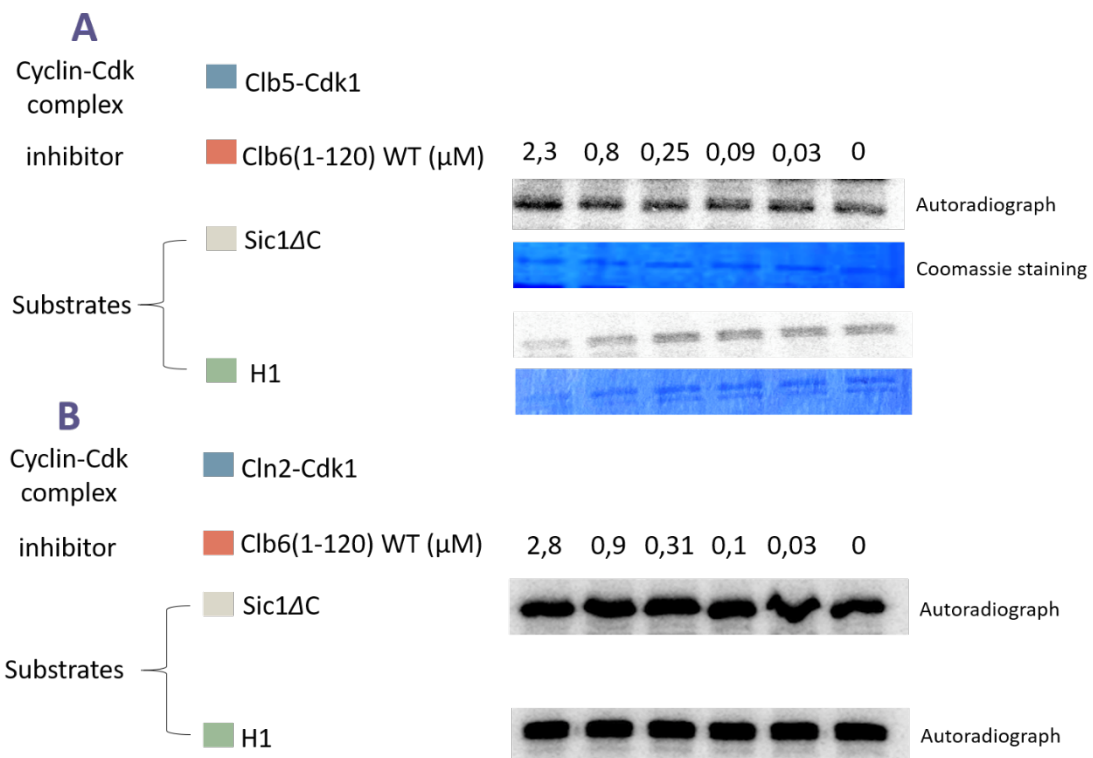


Figure 8. Inhibitory kinase assays. Aliquots of reaction mixtures were collected 14 minutes after the initiation of phosphorylation. The concentrations (μ M) of Clb6(1-120) used for inhibition are indicated above every lane. Autoradiograph and Coomassie stained polyacrylamide gels are shown.

3.2.4 Deletion of *clb5* results in prolonged presence of Clb6 in cells

To study Clb6 oscillations *in vivo*, an endogenous copy of *CLB6* was tagged with 6xHA. Cells were synchronized in G1 via α -factor arrest, released from arrest, and followed for 75 minutes. Aliquots of 11 timepoints were collected and the level of Clb6 was analyzed with Western blotting. To determine if Clb5-Cdk1 affects Clb6 levels, WT and *clb5 Δ* strains were used (**Figure 9, A and B**). Clb6 levels in the WT strain reach a peak at 25 minutes after α -factor release and then get rapidly degraded within 5-10 afterwards. On the other hand, deletion of *CLB5* led to a decreased Clb6 levels and a prolonged degradation profile. This may be due to the fact that cells lacking Clb5 have an extended S phase (Jackson *et al.*, 2006), or it might hint at the transcriptional regulation of *CLB6* by Clb5-Cdk1.

Next, a strain was created, where *CLB5* was substituted with *CLB2* and Clb2 inhibitor Swe1 deleted (*clb5 Δ ::CLB2 swe1 Δ*). Clb2-Cdk1 complex has a higher intrinsic activity than Clb5-Cdk1. This strain allowed to check if higher intrinsic activity of Cdk1 was enough to trigger Clb6 degradation. This result may suggest that the presence of Clb2 at the same time with Clb6 can lead to destabilization of Clb6 (**Figure 9, C**). However, Clb2 may repress *CLB6* transcription as it was previously shown that Clb2-Cdk1 may inhibit SBF and MBF transcription factors responsible for the expression of *CLB6* (Koch *et al.*, 1996).

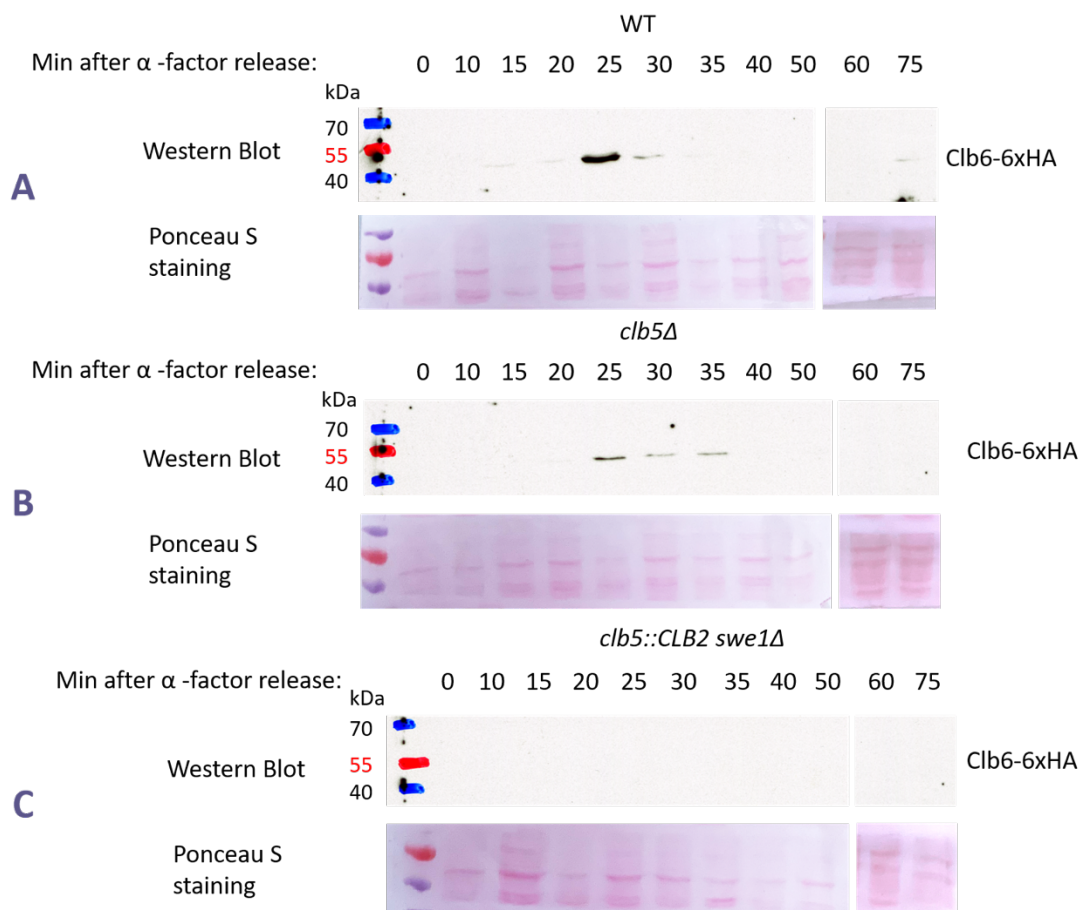


Figure 9. Western blots with corresponding Ponceau S staining of strains analyzed. Time of aliquot collection is relative to α -factor release (minutes). **A.** Wild-type strain (WT). **B.** CLB5 deletion strain (*clb5Δ*). **C.** Strain, where *CLB5* is substituted with *CLB2* and Clb2 inhibitor Swe1 deleted (*clb5Δ::CLB2 swe1Δ*). 3 independent experiments were performed and illustrative one is shown.

3.2.5 Clb6-Cdk1 might phosphorylate itself *in trans* and trigger Clb6 degradation.

To check how Clb6 levels fluctuate during the cell cycle on a single cell scale, time-lapse microscopy experiments were performed. Fusion proteins that consist of one of the Clb6 variants (full length, 1-100 aa, or 1-120 aa), fluorescent marker mCitrine, and the nuclear localization signal (NLS) were created and expressed from the strong inducible promoter LexA. This promoter is controlled by the orthogonal transcription factor LexA-ER-AD that requires β -estradiol for its activation (Ottoz *et al.*, 2014). Transcriptional repressor Whi5 was fused to fluorescent reporter mCherry. Fluorescent signal of mCherry was followed to

track the cell cycle phase since Whi5 nuclear export indicates the transition to the S phase (Start point).

Clb6 with different combinations of mutated putative regulatory elements were created:

1. Wild-type version of Clb6 (WT);
2. S6 and S9 mutated to alanine (S6A S9A);
3. S9 mutated to alanine and KEN box and D-box motifs disrupted (S9A KEN box D-box);
4. T39 mutated to alanine (T39A);
5. S6, S9 mutated to alanine and KEN-box and D-box motifs disrupted (S6A S9A KEN box D-box);
6. Clb6 with disrupted KEN-box and D-box motifs (KEN box D-box).

In total, 18 different strains (6 variants of every size) were investigated in time-lapse microscopy. The expression of Clb6 fusion proteins was induced with 500 nM β -estradiol and cells were followed for 8 hours. Microscopic images of phase-contrast and fluorescent channels were taken every 3 minutes. Exported images were quantified using MATLAB software. To align cells according to the cell cycle phase, 50% nuclear export of the Whi5 was used as a synchronization point.

The results indicate that levels of the full-length versions of Clb6 stay low throughout the cell cycle (**Figure 10**). Full length Clb6 fusion is able to bind Cdk1 and form the active Cyclin-Cdk1 complex. This binding increases the local concentration of Clb6 near Cdk1. Since Cdk1 was previously shown to phosphorylate Clb6 *in vitro* (Cross *et al.*, 2002), it is possible that Clb6 is autophosphorylated *in trans* by Clb6-Cdk1.

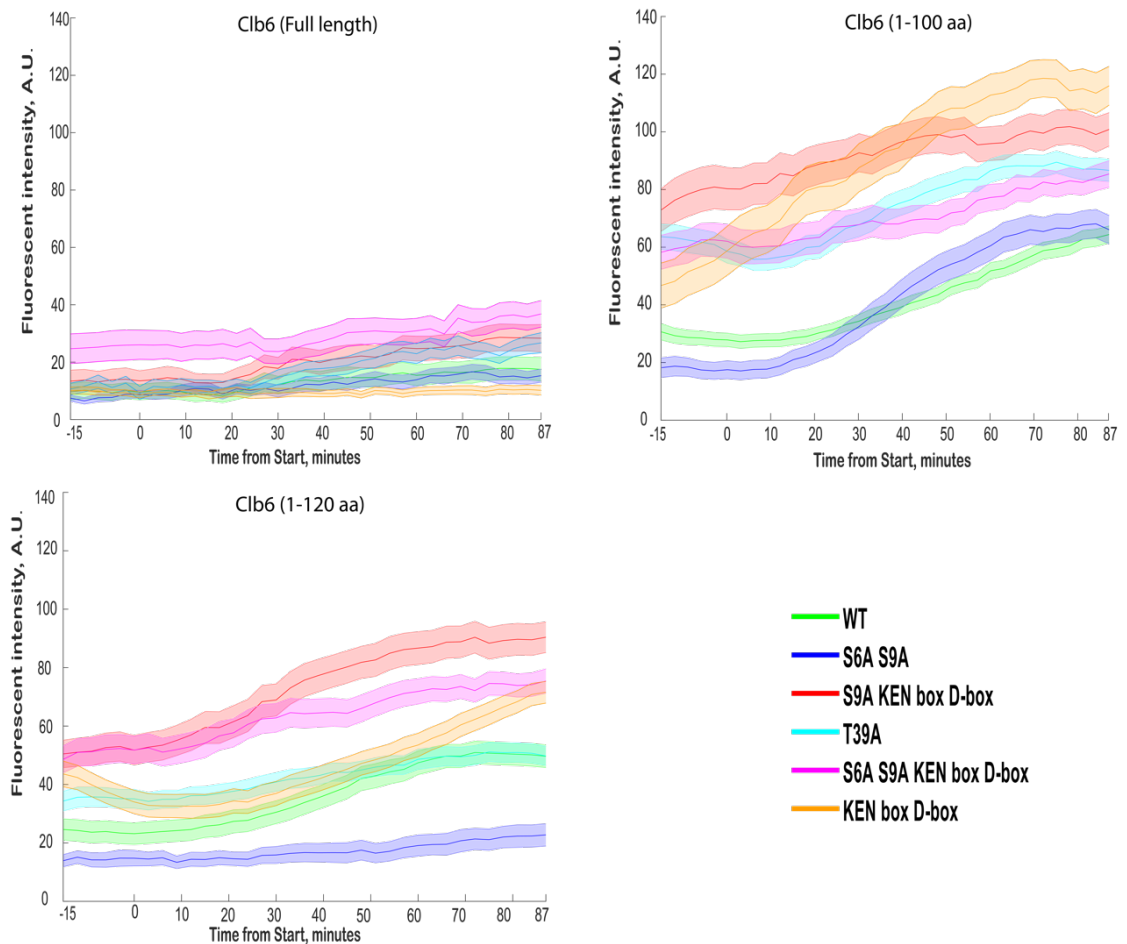


Figure 10. Time-lapse microscopy. X-axis represents the minutes from the Whi5 nuclear export (Start point). On Y-axis the intensity of the fluorescence is indicated in arbitrary units (A.U.). Lines represent the average intensity of the mCitrine signal, shaded error bars represent the standard error of the mean. Around 50 individual cells were used for the analysis.

In truncated versions, mutations of S6 and S9 to alanine do not cause Clb6 stabilization, KEN box and D-box mutations lead to elevated levels of Clb6, and S6A S9A KEN box D-box mutants behave similarly to only KEN box D-box mutants. Mutation of T39 phosphorylation site to alanine does not cause substantial stabilization effect. Altogether, these results suggest that IPSPIS phospho-degron motif is not essential for Clb6 degradation and mutation of T39 alone is not stabilizing Clb6.

The levels of cyclins depend on both transcriptional and post-translational regulation. It was recently shown that the mRNA of *CLB6* is less stable compared to other B-type cyclins and contains instability elements in both coding sequence and 3' untranslated region (3' UTR). The deletion of the gene responsible for mRNA degradation (*ccr4Δ*) leads to an increase in both *CLB6* mRNA and Clb6 protein levels (Cocuangco Revilleza *et al.*, 2022). This could partially explain the shorter time-window of Clb6 appearance, however, does not shine a light on the Clb6 degradation mechanism.

The results of this work demonstrate that among Cln2, Clb5, Clb6, and Clb2 only Clb6-Cdk1 was able to phosphorylate Clb6(1-120) with some degree of efficiency *in vitro*. This result contradicts previously published data, where Cln2-Cdk1 was also shown to phosphorylate Clb6 in *in vitro* ³⁵S-Methionine-mediated kinase assays (Wu *et al.*, 2016). There, electrophoretic shift was measured to determine phosphorylation state of the Clb6. However, different phosphorylation sites may cause higher shifts compared to others, and some do not cause any. Therefore, the phosphorylation assays performed in this study are more quantitative, as they directly indicate radioactive phosphoryl group incorporation into the substrates.

In addition to Cdk1, other kinases are required for efficient degradation of Clb6. Pho85, another cyclin-dependent kinase, has been shown to phosphorylate Clb6 *in vitro* and has a minor effect on its stability *in vivo*. Moreover, inactivation of both Cdk1 and Pho85 stabilizes Clb6 substantially (Jackson *et al.*, 2006; Wu *et al.*, 2016), supporting the idea of phosphorylation dependent Clb6 degradation.

The results of time-lapse microscopy experiments indicate that putative IPSPIS Cdc4 phospho-degron motif is not essential for Clb6 degradation, and confirm the functionality of APC degrons (KEN box and D-box). Thus, the exact mechanism of phosphorylation-dependent degradation remains unclear and further research is required to uncover the phospho-regulation of Clb6 stability.

SUMMARY

Cyclins appear in cells periodically as they are expressed and degraded in pulses. They are responsible for cyclin-dependent kinase activation, and they mediate the substrate targeting of the Cdk1 complex. B-type cyclins Clb5 and Clb6 are expressed at the end of the G1 phase but are degraded at different timepoints. Clb5, along with other B-type cyclins Clb1-4, contains APC degnon motifs and is degraded in the M phase. Clb6, on the other hand, is rapidly degraded already in the S phase. N-terminal truncations of Clb6 have previously been shown to stabilize this cyclin, leading to the idea that regulatory elements are present there.

The amino acid analysis of Clb6 showed the potential regulatory sequences present in the N-terminus. A putative Cdc4 phospho-degnon motif was spotted at positions 4-9, APC degnon motifs KEN box and D-box (at positions 23-25 and 64-72, respectively), and putative Clb5-specific docking motif DPF at positions 113-115.

In this study, we investigated if these putative regulatory regions might be responsible for Clb6 degradation. We also determined which Cyclin-Cdk1 complex can phosphorylate the N-terminal part of Clb6 and studied Clb6 levels in different background strains *in vivo* with time-lapse microscopy and western blotting.

Our results indicate that the proposed phospho-degnon motif (IPSPIS, positions 4-9) is not essential for control of Clb6 levels, since mutations of S6 and S9 phosphorylation sites do not lead to Clb6 stabilization. However, previous studies indicate that Clb6 degradation is phosphorylation dependent leading to the idea that other phosphorylation site(s) (e.g., S147) may regulate degradation of Clb6. Our microscopy data suggests that APC degnon motifs are functional in Clb6, however, their mutations do not lead to Clb6 stabilization in case of full length Clb6. This suggests that multiple mechanisms compensatory involving both APC and SCF could mediate degradation of full-length Clb6.

In vitro kinase assay experiments showed that the N-terminal part of Clb6 (Clb6(1-120)) is most rapidly phosphorylated by Clb6-Cdk1 compared to Cln2-, Clb5-, Clb2-Cdk1 leading to the hypothesis that Clb6 might autophosphorylate itself *in trans*.

The analysis of *in vivo* experiments indicates that in the absence of Clb5, Clb6 levels are lower but stay stable for a longer period compared to the wild-type cells with Clb5. As S phase is considerably prolonged in *clb5Δ* cells, this indicates that there could be a feedback mechanism between S phase progression and Clb6 degradation.

To conclude, the exact mechanism of Clb6 degradation remain unclear and further research is needed to determine how Clb6 levels in the cells are regulated.

REFERENCES

- Ang, X. L., & Harper, J. W. (2005). SCF-mediated protein degradation and cell cycle control. *Oncogene*, *24*, 2860–2870. <https://doi.org/10.1038/sj.onc.1208614>
- Bandyopadhyay, S., Bhaduri, S., Örd, M., Davey, N. E., Loog, M., & Pryciak, P. M. (2020). Comprehensive Analysis of G1 Cyclin Docking Motif Sequences that Control CDK Regulatory Potency In Vivo. *Current Biology*, *30*(22), 4454–4466.e5. <https://doi.org/10.1016/J.CUB.2020.08.099>
- Barford, D. (2011). Structure, function and mechanism of the anaphase promoting complex (APC/C). *Quarterly Reviews of Biophysics*, *44*(2), 153–190. <https://doi.org/10.1017/S0033583510000259>
- Barnum, K. J., & O’Connell, M. J. (2014). Cell cycle regulation by checkpoints. *Methods in Molecular Biology*, *1170*, 29–40. https://doi.org/10.1007/978-1-4939-0888-2_2
- Bäumer, M., Braus, G. H., & Irniger, S. (2000). Two different modes of cyclin Clb2 proteolysis during mitosis in *Saccharomyces cerevisiae*. *FEBS Letters*, *468*(2–3), 142–148. [https://doi.org/10.1016/S0014-5793\(00\)01208-4](https://doi.org/10.1016/S0014-5793(00)01208-4)
- Bloom, J., & Cross, F. R. (2007a). Multiple levels of cyclin specificity in cell-cycle control. *Nature Reviews Molecular Cell Biology* 2007 8:2, *8*(2), 149–160. <https://doi.org/10.1038/nrm2105>
- Bloom, J., & Cross, F. R. (2007b). Multiple levels of cyclin specificity in cell-cycle control. *Nature Reviews Molecular Cell Biology* 2007 8:2, *8*(2), 149–160. <https://doi.org/10.1038/nrm2105>
- Brown, N. R., Noble, M. E. M., Endicott, J. A., & Johnson, L. N. (1999). The structural basis for specificity of substrate and recruitment peptides for cyclin-dependent kinases. *Nature Cell Biology* 1999 1:7, *1*(7), 438–443. <https://doi.org/10.1038/15674>
- Cocuangco Revilleza, J. E., Sato, M., Irie, K., Suda, Y., Mizuno, T., & Irieid, K. (2022). Regulation of CLB6 expression by the cytoplasmic deadenylase Ccr4 through its coding and 3’ UTR regions. *PLOS ONE*, *17*(5), e0268283. <https://doi.org/10.1371/JOURNAL.PONE.0268283>

- Cross, F. R., Archambault, V., Miller, M., & Klovstad, M. (2002). Testing a mathematical model of the yeast cell cycle. *Molecular Biology of the Cell*, *13*(1), 52–70. <https://doi.org/10.1091/MBC.01-05-0265>
- Donaldson, A. D., Raghuraman, M. K., Friedman, K. L., Cross, F. R., Brewer, B. J., & Fangman, W. L. (1998). CLB5-dependent activation of late replication origins in *S. cerevisiae*. *Molecular Cell*, *2*(2), 173–182. [https://doi.org/10.1016/S1097-2765\(00\)80127-6](https://doi.org/10.1016/S1097-2765(00)80127-6)
- Doncic, A., Eser, U., Atay, O., & Skotheim, J. M. (2013). An Algorithm to Automate Yeast Segmentation and Tracking. *PLOS ONE*, *8*(3), e57970. <https://doi.org/10.1371/JOURNAL.PONE.0057970>
- Enserink, J. M., & Kolodner, R. D. (2010). An overview of Cdk1-controlled targets and processes. In *Cell Division* (Vol. 5). <https://doi.org/10.1186/1747-1028-5-11>
- Faustova, I., Bulatovic, L., Matiyevskaya, F., Valk, E., Örd, M., & Loog, M. (2021). A new linear cyclin docking motif that mediates exclusively S-phase CDK-specific signaling. *The EMBO Journal*, *40*(2). <https://doi.org/10.15252/embj.2020105839>
- Feldman, R. M. R., Correll, C. C., Kaplan, K. B., & Deshaies, R. J. (1997). A complex of Cdc4p, Skp1p, and Cdc53p/cullin catalyzes ubiquitination of the phosphorylated CDK inhibitor Sic1p. *Cell*, *91*(2), 221–230. [https://doi.org/10.1016/S0092-8674\(00\)80404-3](https://doi.org/10.1016/S0092-8674(00)80404-3)
- Geymonat, M., Spanos, A., Wells, G. P., Smerdon, S. J., & Sedgwick, S. G. (2004). Clb6/Cdc28 and Cdc14 Regulate Phosphorylation Status and Cellular Localization of Swi6. *Molecular and Cellular Biology*, *24*(6), 2277–2285. <https://doi.org/10.1128/mcb.24.6.2277-2285.2004>
- Gnügge, R., Liphardt, T., & Rudolf, F. (2016). A shuttle vector series for precise genetic engineering of *Saccharomyces cerevisiae*. *Yeast (Chichester, England)*, *33*(3), 83–98. <https://doi.org/10.1002/YEA.3144>
- Haase, S. B., Winey, M., & Reed, S. I. (2001). Multi-step control of spindle pole body duplication by cyclin-dependent kinase. *NATURE CELL BIOLOGY*, *3*. <http://cell-bio.nature.com38>

- Jackson, L. P., Reed, S. I., & Haase, S. B. (2006). Distinct Mechanisms Control the Stability of the Related S-Phase Cyclins Clb5 and Clb6. *Molecular and Cellular Biology*, 26(6), 2456–2466. <https://doi.org/10.1128/mcb.26.6.2456-2466.2006>
- Janke, C., Magiera, M. M., Rathfelder, N., Taxis, C., Reber, S., Maekawa, H., Moreno-Borchart, A., Doenges, G., Schwob, E., Schiebel, E., & Knop, M. (2004). Yeast Functional Analysis Report A versatile toolbox for PCR-based tagging of yeast genes: new fluorescent proteins, more markers and promoter substitution cassettes. *Yeast*, 21, 947–962. <https://doi.org/10.1002/yea.1142>
- Koch, C., Schleiffer, A., Ammerer, G., & Nasmyth, K. (1996). Switching transcription on and off during the yeast cell cycle: Cln/Cdc28 kinases activate bound transcription factor SBF (Swi4/Swi6) at start, whereas Clb/Cdc28 kinases displace it from the promoter in G2. *Genes & Development*, 10(2), 129–141. <https://doi.org/10.1101/GAD.10.2.129>
- Kõivomägi, M., Örd, M., Iofik, A., Valk, E., Venta, R., Faustova, I., Kivi, R., Balog, E. R. M., Rubin, S. M., & Loog, M. (2013). Multisite phosphorylation networks as signal processors for Cdk1. *Nature Structural & Molecular Biology*, 20(12), 1415–1424. <https://doi.org/10.1038/NSMB.2706>
- Kõivomägi, M., Valk, E., Venta, R., Iofik, A., Lepiku, M., Morgan, D. O., & Loog, M. (2011). Dynamics of Cdk1 Substrate Specificity during the Cell Cycle. *Molecular Cell*, 42(5), 610–623. <https://doi.org/10.1016/j.molcel.2011.05.016>
- Kõivomägi, M., Valk, E., Venta, R., Iofik, A., Lepiku, M., Rose, E., Balog, M., Rubin, S. M., Morgan, D. O., & Loog, M. (2011). Cascades of multisite phosphorylation control Sic1 destruction at the onset of S phase. *Nature*, 480. <https://doi.org/10.1038/nature10560>
- Loog, M., & Morgan, D. O. (2005). Cyclin specificity in the phosphorylation of cyclin-dependent kinase substrates. *Nature*, 434(7029), 104–108. <https://doi.org/10.1038/NATURE03329>
- Morgan, D. O. (2007). Cell Cycle: Principles of Control. *The Yale Journal of Biology and Medicine*, 80(3).

- Örd, M., & Loog, M. (2019). How the cell cycle clock ticks. In *Molecular Biology of the Cell* (Vol. 30, Issue 2, pp. 169–172). American Society for Cell Biology. <https://doi.org/10.1091/mbc.E18-05-0272>
- Örd, M., Puss, K. K., Kivi, R., Möll, K., Ojala, T., Borovko, I., Faustova, I., Venta, R., Valk, E., Kõivomägi, M., & Loog, M. (2020). Proline-Rich Motifs Control G2-CDK Target Phosphorylation and Priming an Anchoring Protein for Polo Kinase Localization. *Cell Reports*, 31(11). <https://doi.org/10.1016/J.CELREP.2020.107757>
- Örd, M., Venta, R., Möll, K., Valk, E., & Loog, M. (2019). Cyclin-Specific Docking Mechanisms Reveal the Complexity of M-CDK Function in the Cell Cycle. *Molecular Cell*, 75(1), 76-89.e3. <https://doi.org/10.1016/J.MOLCEL.2019.04.026>
- Ottoz, D. S. M., Rudolf, F., & Stelling, J. (2014). Inducible, tightly regulated and growth condition-independent transcription factor in *Saccharomyces cerevisiae*. *Nucleic Acids Research*, 42(17), e130. <https://doi.org/10.1093/NAR/GKU616>
- Pines, J. (1995). Cyclins and cyclin-dependent kinases: a biochemical view. In *Biochem. J* (Vol. 308).
- Richardson, H. E., Wittenberg, C., Cross, F., & Reed, S. I. (1989). An essential G1 function for cyclin-like proteins in yeast. *Cell*, 59(6), 1127–1133. [https://doi.org/10.1016/0092-8674\(89\)90768-X](https://doi.org/10.1016/0092-8674(89)90768-X)
- Schulman, B. A., Lindstrom, D. L., & Harlow, E. (1998). Substrate recruitment to cyclin-dependent kinase 2 by a multipurpose docking site on cyclin A. *Proceedings of the National Academy of Sciences of the United States of America*, 95(18), 10453–10458. <https://doi.org/10.1073/PNAS.95.18.10453>
- Schwob, E., & Nasmyth, K. (n.d.). *CLB5 and CLB6, a new pair of B cyclins involved in DNA replication in Saccharom yces cereHsiae*.
- Shirayama, M., Tóth, A., Gálová, M., & Nasmyth, K. (1999). APCCdc20 promotes exit from mitosis by destroying the anaphase inhibitor Pds1 and cyclin Clb5. *Nature* 1999 402:6758, 402(6758), 203–207. <https://doi.org/10.1038/46080>

- Skowyra, D., Craig, K. L., Tyers, M., Elledge, S. J., & Harper, J. W. (1997). F-Box Proteins Are Receptors that Recruit Phosphorylated Substrates to the SCF Ubiquitin-Ligase Complex. *Cell*, *91*(2), 209–219. [https://doi.org/10.1016/S0092-8674\(00\)80403-1](https://doi.org/10.1016/S0092-8674(00)80403-1)
- Venta, R., Valk, E., Örd, M., Košik, O., Pääbo, K., Maljavin, A., Kivi, R., Faustova, I., Shtaida, N., Lepiku, M., Möll, K., Doncic, A., Kõivomägi, M., & Loog, M. (2020). A processive phosphorylation circuit with multiple kinase inputs and mutually divergent routes controls G1/S decision. *Nature Communications* *2020 11:1*, *11*(1), 1–14. <https://doi.org/10.1038/s41467-020-15685-z>
- Verma, R., McDonald, H., Yates, J. R., & Deshaies, R. J. (2001). Selective Degradation of Ubiquitinated Sic1 by Purified 26S Proteasome Yields Active S Phase Cyclin-Cdk. *Molecular Cell*, *8*(2), 439–448. [https://doi.org/10.1016/S1097-2765\(01\)00308-2](https://doi.org/10.1016/S1097-2765(01)00308-2)
- Wu, S. Y., Kuan, V. J. W., Tzeng, Y. W., Schuyler, S. C., & Juang, Y. L. (2016). The anaphase-promoting complex works together with the SCF complex for proteolysis of the S-phase cyclin Clb6 during the transition from G1 to S phase. *Fungal Genetics and Biology*, *91*, 6–19. <https://doi.org/10.1016/J.FGB.2016.03.004>

NON-EXCLUSIVE LICENCE TO REPRODUCE THESIS AND MAKE THESIS PUBLIC

I, Avishan Aghayari,

1. herewith grant the University of Tartu a free permit (non-exclusive licence) to reproduce, for the purpose of preservation, including for adding to the DSpace digital archives until the expiry of the term of copyright,

“Analysis of Clb6 degradation mechanisms”,

supervised by Ilona Faustova, Artemi Maljavin

2. I grant the University of Tartu the permit to make the thesis specified in point 1 available to the public via the web environment of the University of Tartu, including via the DSpace digital archives, under the Creative Commons licence CC BY NC ND 4.0, which allows, by giving appropriate credit to the author, to reproduce, distribute the work and communicate it to the public, and prohibits the creation of derivative works and any commercial use of the work from **27/05/2025** until the expiry of the term of copyright,

3. I am aware of the fact that the author retains the rights specified in p. 1 and 2.

4. I certify that granting the non-exclusive licence does not infringe other persons' intellectual property rights or rights arising from the personal data protection legislation.

Avishan Aghayari

27/05/2022